# Influence of the grain boundary network on the critical current density of deformation-textured YBa$_2$Cu$_3$O$_{7-x}$ coated conductors made by metal-organic deposition

S. I. Kim,[1] D. M. Feldmann,[1] D. T. Verebelyi,[2] C. Thieme,[2] X. Li,[2] A. A. Polyanskii,[1] and D. C. Larbalestier[1]

[1]*Applied Superconductivity Center, University of Wisconsin, Madison, Wisconsin 53706, USA*

[2]*American Superconductor Corporation, Westborough, Massachusetts 01581, USA*

Coated conductors (CC) are quasisingle crystals consisting of a series-parallel network of predominantly low angle grain boundaries, whose network misorientation distribution determines the current-carrying characteristics. To deepen our understanding of the influence of the grain boundary network in CC, we present a study of critical current density ($J_c$) and electric field–current density ($E$-$J$) characteristics over a broad range of magnetic fields and temperatures in a series of three 1-µm-thick YBa$_2$Cu$_3$O$_{7-x}$ samples with variable textures, including a single-crystal film and two deformation-textured coated conductors made by a metal-organic deposition (MOD) process. We also investigated the influence of the number of grains within the bridge width by successively narrowing the bridge on the better-textured CC. We found clear evidence of crossover from grain boundary (GB) network control to grain control of $J_c$ by study of the magnitude of $J_c$ and the shape of the $E$-$J$ characteristic. In the narrowest tracks, we were able to isolate the effect of single GBs, finding dissipation only when the misorientation exceeded $\sim 7°$, more than twice that seen in classic bicrystal experiments. We found that the influence of global texture on $J_c$ (77 K, 0 T) is highly nonlinear, $J_c$ rising by more than 2.5 times as the full width at half maximum decreases only by $\sim 2°$. Very interestingly, the MOD-CC exhibited no grain boundary dissipation signature in their $E$-$J$ characteristics in wide bridges, showing that global influence of grain boundary network is very much attenuated even for the grain boundary network containing misorientations that would generate significant dissipation in thin film bicrystals.

## I. INTRODUCTION

Grain boundaries (GBs) of YBa$_2$Cu$_3$O$_{7-x}$ (YBCO) are well known as regions of weakened superconductivity. They are structurally and compositionally heterogeneous on scales of 1–5 nm, comparable to that of the coherence length, $\xi$. Low angle GBs consist of GB dislocations separated by conductive, grainlike channels.[1] The atomic disruptions and strain fields of the core depress the superconducting order parameter[1,2] and, thus, depress the supercurrent density. At small angles, e.g., 5° of [001] tilt, dislocation cores are separated by $\sim 4$ nm, so the channel can be more than $\xi_{ab}$ ($\sim 3.5$ nm at 77 K) wide but the GB dislocation separation decreases inversely with increasing misorientation angle, $\theta$, so that at about 10° the disruptive effects of strain and disorder close the channel. An important and poorly understood component of the disruption is loss of oxygen as means of minimizing the GB strain, which additionally weakens superconductivity across the GBs.[3,4] Wider oxygen-depleted regions have been seen at higher misorientations, exacerbating the weak coupling across the GB.[3,4]

Suppressed superconductivity at the GB causes a reduced critical current density ($J_c$). It has been well established from [001] tilt bicrystal experiments[5–7] and microbridge experiments on coated conductors[8] (CCs) that $J_c$ of GBs decreases exponentially with increasing misorientation angle ($\theta$), falling below that of the grain beyond a critical angle ($\theta_c$) of 3°–4°. However, it is also becoming clear that $\theta_c$ is both field and temperature dependent,[8–10] although so far $\theta_c$ is determined only at self-field.

Not only are $J_c$ values across the GB depressed but so also do the vortex properties change, as is apparent in the voltage-current ($V$-$I$) characteristics. Typical $V$-$I$ characteristics within the grain exhibit rather straight and evenly spaced traces when plotted in log-log $V$-$I$ space.[10] However, $V$-$I$ characteristics for a GB with $\theta > \theta_c$ show a steep rise in $V$ and a "knee" at higher voltage in a log-log $V$-$I$ plot, while showing non-Ohmic linear differential (NOLD) behavior in a linear $V$-$I$ plot. The steep voltage rise in the log-log $V$-$I$ plot is a characteristic GB dissipation signature, caused by depinning of hybrid Abrikosov-Josephson vortices in the GB.[11] Such characteristics are clearly evident in many classical bicrystal experiments[6,7,9,10] in which the YBCO grain boundary grows parallel to the $c$ axis. The GB very effectively captures vortices when field is applied along this axis too.

The nature of the GB dissipation depends on both magnetic and electric field. In intermediate magnetic fields the $V$-$I$ traces across a single GB often show hybrid behavior, in which there is grainlike dissipation at low voltage levels followed by a steep rise characteristic of depinning of the GB vortices at midvoltage levels, followed by a knee which makes the transition to broad flux flow dissipation in the grains at higher voltage levels.[10] The $V$-$I$ traces become more grainlike in higher magnetic fields as the GB dissipation signature disappears and flux flow in the grains dominates. It is gradually becoming clear that the crossover field at which the grain starts to dissipate prior to the GB dissipation depends on misorientation angle. For a 7° bicrystal, the crossover field is between 5 and 6 T at 77 K as shown in Gurevich *et al.*[11] Verebelyi *et al.*[7] found that the crossover field is around 4 T for a 3.8° GB and 0 T for a 2.0° ($< \theta_c$) GB while Holzapfel *et al.*[12] found a cross-

over field of 1 T for a 4° GB, 4 T for an 8° GB, and 6 T for a 12° GB.

The GB superconducting properties are affected by temperature too. Polyanskii *et al.* found by low field (~0.1 T) magneto-optic study[13] that $J_c(T)$ of low angle GBs with 3°–10° are less temperature dependent than $J_c(T)$ in the grain and thus that the difference between $J_c$ of the grains and $J_c$ of the GBs becomes less pronounced at higher temperature. In summary, we can say that studies of single low-angle GBs shows that they become more single-crystal-like as temperature and magnetic field increases and that $\theta_c$ is also thus dependent on temperature and magnetic field.

How this diversity of GB behavior controls the $J_c$ of CCs is both interesting and technologically important. CCs are quasi-single crystals consisting of a series-parallel network of predominantly low angle GBs, whose global properties result from series-parallel, multipath percolative current transport.[14,15] The most practical way to evaluate the grain misorientation of CCs over large length scales is by x-ray diffraction pole figures, from which the full width half maximum (FWHM) of both in-plane ($\Delta\phi$) and out-of-plane ($\Delta\omega$) misorientations can be determined. However, it is the grain-to-grain misorientation which actually determines the local intergranular current density. Although this local misorientation matrix can be determined by electron backscattering diffraction (EBSD) analysis, it is not feasible to do this on scales larger than about 1 mm$^2$. Numerical simulations of the global $J_c$ of CCs have been addressed by various models,[16–18] which include the influence of the degree of texture, the number of grains in the tape width, and tape length. Such models indeed show that $J_c$ values are reduced with worsening texture and decreasing number of grains within the tape width. However, such models suffer from a certain quantitative imprecision because the range of texture found in present CCs (FWHM of ~4°–8°) lies exactly within the same range that the GB misorientation obstructs the current.

Based on the simplest analogy of a CC to the known properties of single GBs in bicrystals, we would expect that $J_c$ of CCs would be reduced as the texture worsens and that GB effects would become less pronounced as field and temperature rise. Consistent with this expectation, Fernandez *et al.*[19] found that a CC with a YBCO in-plane FWHM of 8° exhibited both significantly reduced $J_c$ values compared to those expected from the intragranular behavior and a distinctive GB dissipation signature in the V-I characteristics below 4 T at 77 K, while showing no GB limitation of $J_c$ beyond 4 T at 77 K. They also reported that this GB-to-grain crossover field became progressively larger as the temperature decreased, consistent with the magneto-optical study of GB effects by Polyanskii *et al.*[13] They clearly established that the domain within which the GB reduced $J_c$ depended strongly on the temperature and magnetic field.

The purpose of the present paper is to deepen our understanding of the influence of global texture on the critical current density using two recent CCs with smaller FWHM than that studied by Fernandez *et al.*[19] We amplified our study by cutting progressively narrower tracks into the better textured CC so as to observe changes in $J_c(H,T)$ behavior as the conductor moved from many grains to about one grain in width. We compare these results to a similarly made YBCO film grown on a single crystal substrate. The layout of our paper is as follows. Section II describes the experimental details. In Sec. III, we contrast three nominal 1-μm-thick films with different textures by using broad-range measurements of $J_c(H,T)$ and electric field–current density (E-J) characteristics. Then, in Sec. IV, the influence of the number of grains in the track width is explored by contrasting the transport behaviors of different bridge widths on the better-textured CC sample. In the discussion of Sec. V we show how our study delineates the influence of the grain boundary network in controlling the $J_c$ properties at lower field and temperature, transitioning to a grain-dominated regime at higher fields and temperatures.

## II. EXPERIMENTAL DETAILS

All three nominal 1-μm-thick YBCO films were grown using the same *ex situ* trifluoroacetate (TFA)-based precursor metal-organic deposition (MOD) process.[20,21] The precursor was deposited by solution coating and then decomposed to BaF$_2$, CuO, and Y$_2$O$_3$ which were then continuously converted to the superconducting YBCO phase in a humid, low oxygen partial pressure environment at 700–800 °C.[20,21] The YBCO single crystalline film was grown epitaxially on CeO$_2$-buffered YSZ single crystal using the same MOD process. For the two CC samples, epitaxial buffer layers of Y$_2$O$_3$/YSZ/CeO$_2$ were deposited on the Ni 5 at. %W rolling assisted biaxially textured substrate (RABiTS).

Bridges were defined on the CC samples (~300 μm wide by ~500 μm long) by Nd-YAG (yttrium aluminum garnet) laser ablation, and on the single crystal (30 μm wide by 100 μm long) by photolithography so as to restrict critical current ($I_c$) to <10 A at full thickness. The bridges on the CCs were more than seven grains wide given the observed Ni-W template grain sizes of ~40 μm. The V-I characteristics were obtained with standard four-point measurements. A current pulse of 50 ms duration with 30 ms voltage read was used for currents higher than 100 mA to prevent possible sample heating. The measurements were performed over a wide range of magnetic fields up to 12 T applied perpendicular to the film surface at temperatures of 77, 65, 50, 40, and 27 K. The $J_c$ values were determined using the usual electric field criterion of 1 μV/cm. Although the MOD/TFA process produces a high-$J_c$ YBCO layer, it is also porous with a surface roughness of order about 10% of the thickness, which limits the absolute accuracy of our critical current density numbers to about the same value. The superconducting critical temperature ($T_c$) was determined as the onset of zero resistance.

The effect of the number of grains in the bridge width was investigated with the better textured CC. Bridges were initially defined by laser cutting tracks ~400 μm wide by ~1 mm long, after which the bridges were successively narrowed to around 50 μm width, about the grain size. To check the local GB misorientation distribution within the bridges, orientation mapping by EBSD was performed. Due to the surface roughness, we could not get good EBSD patterns from the YBCO and had to do this on the Ni-W after etching

TABLE I. Key results of the measured samples (SC, CC1, CC2) and of L. Fernandez *et al.* (see Ref. 19)].

| Sample no. | $\Delta\phi_{YBCO}$ | $\Delta\omega_{YBCO}$ | Bridge width (μm) | $T_c$ (K) | $J_c$ (77 K, sf) (MA/cm$^2$) | $J_c$ (77 K, 1 T) (MA/cm$^2$) | $H^{cr}$ (77 K) (T) |
|---|---|---|---|---|---|---|---|
| SC | | | 30 | 93 | 5.3 | 0.41 | |
| CC1 | 5.5° | 3.8° | 330 | 91 | 2.4 | 0.36 | 2 |
| CC2 | 6.6° | 6.1° | 300 | 89 | 0.9 | 0.11 | none |
| Ref. 19 | 8° | | 300 | | 0.3 | 0.04 | 4 |

away the oxides. A magneto-optic image was taken on the bridge region by field cooling the sample in a perpendicular field of 60 mT to 10 K. These showed up regions where the GB current density was lower than the grain current density.

Global texture measurements were made by x-ray diffraction. The in-plane texture was determined by the FWHM of the in-plane off-axis ($\phi$) scan of the (103) YBCO peak while the out-of-plane texture was measured from the rocking curve of the (005) YBCO peak.

## III. INFLUENCE OF GLOBAL TEXTURE ON THE CRITICAL CURRENT DENSITY

The key texture properties of the three samples are shown in Table I. The better textured, higher $J_c$ sample (CC1) had

5.5° of in-plane FWHM ($\Delta\phi$) and 3.8° of out-of-plane FWHM ($\Delta\omega$), while the worse textured, lower $J_c$ sample (CC2) had $\Delta\phi$ of 6.6° and $\Delta\omega$ of 6.1°, respectively. The $J_c$ (77 K, 0 T) values are directly correlated to the degree of texture. The single crystal sample (SC) achieved the very high $J_c$ value of 5.3 MA/cm$^2$ at self-field, but $J_c$ (77 K, 0 T) was reduced to 2.4 and 0.9 MA/cm$^2$ for CC1 and CC2, respectively. However, at 1 T and 77 K relative differences in $J_c$ were markedly smaller, values of 0.41, 0.36, and 0.11 MA/cm$^2$ were being observed.

Figure 1 shows $J_c(H)$ of the three samples at 77, 65, 50, 40, and 27 K. Some low-temperature, low-field data do not exist because of our 10 A current limit. The worse textured CC2 ($\Delta\phi \sim 6.6°, \Delta\omega \sim 6.1°$) always had
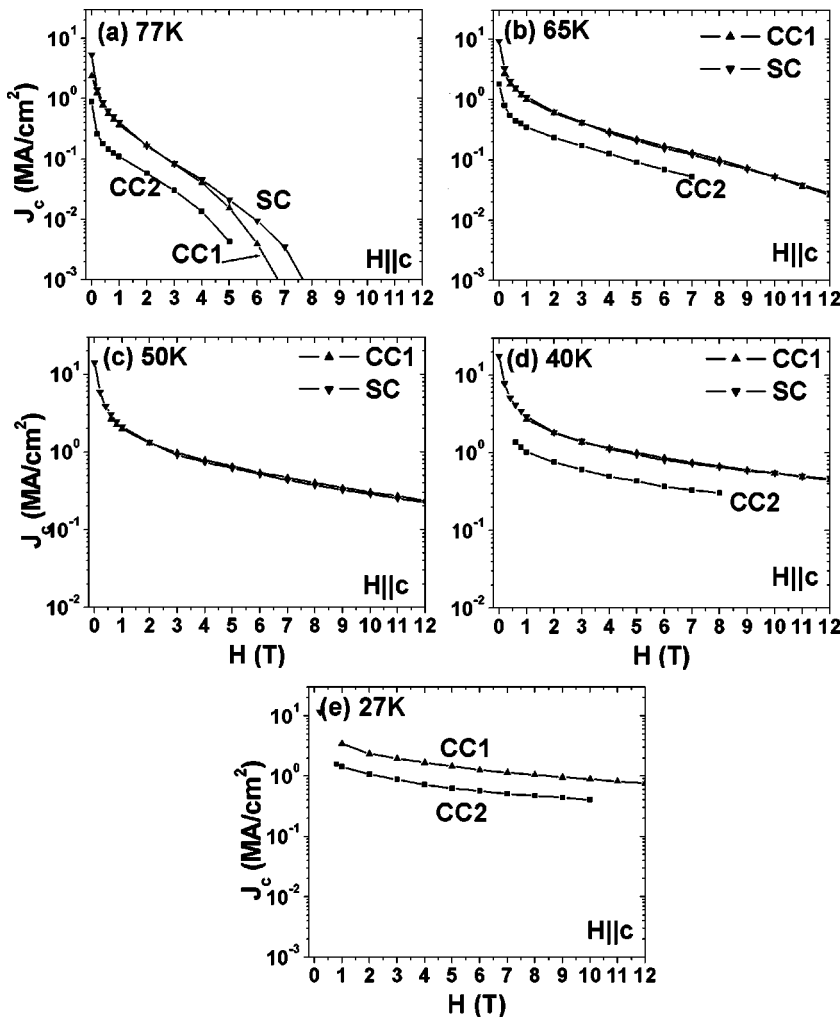


FIG. 1. $J_c(H)$ at variable temperatures (SC, CC1, and CC2); (a) 77, (b) 65, (c) 50, (d) 40, and (e) 27 K. The worse textured CC2 has significantly lower $J_c$ values, in strong contrast to CC1 and SC, which showed very similar $J_c(H)$. Note that $J_c(H)$ of CC1 falling faster than that of SC at 77 K because of the $T_c$ difference.
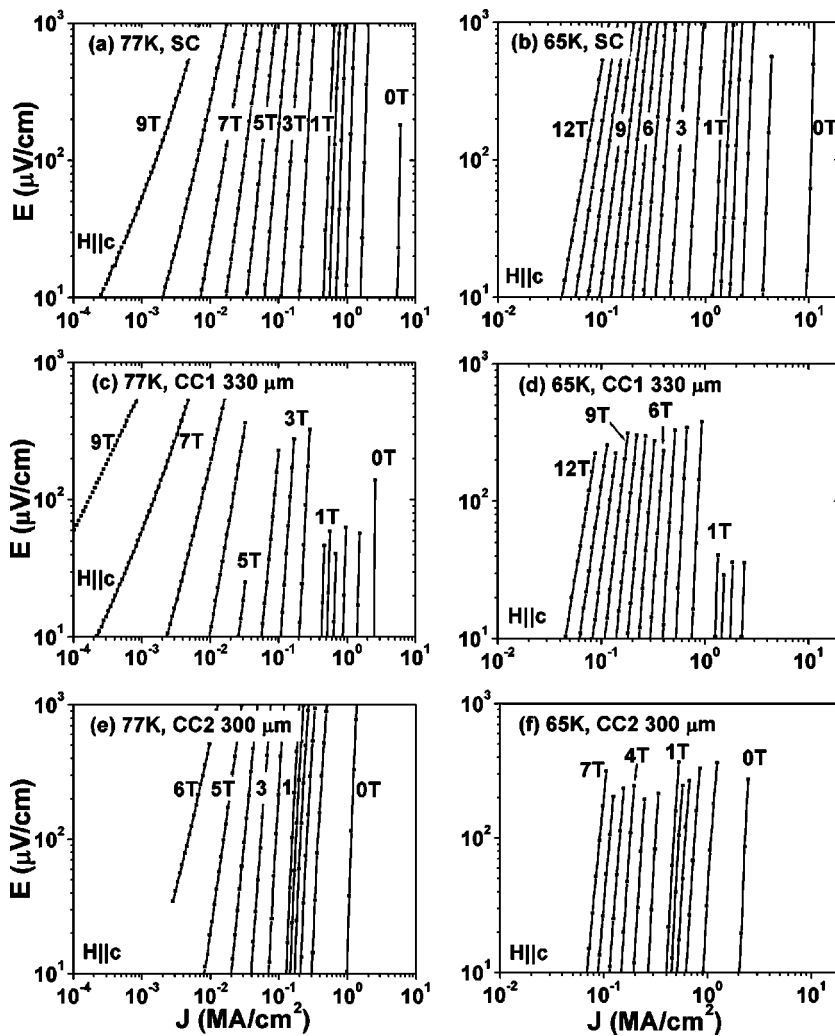
FIG. 2. *E-J* characteristics of (a),(b) SC; (c),(d) CC1; (e),(f) CC2 at (a),(c),(e) 77 and (b),(d),(f) 65 K. The three samples show very similar single-crystal-like *E-J* characteristics in terms of their curve shape and their field dependence even for CC2 that has significantly lower $J_c$ values.

significantly lower $J_c$ values, in strong contrast to CC1 ($\Delta\phi \sim 5.5°$, $\Delta\omega \sim 3.8°$) and SC, which showed very similar $J_c(H)$ behavior over a large range of field ($H$) and temperature ($T$). At 65, 50, and 40 K, CC1 exhibits reduced $J_c$ with respect to SC only at low fields. An interesting feature of Fig. 1 is the parallel field dependence of $J_c(H)$ for all three samples in fields above a few Tesla. Only close to the irreversibility field at 77 K do the $J_c(H)$ curves differ. CC2 has about half the $J_c$ of the SC and CC1 in high fields. It is striking that the differences in $J_c(H)$ between SC and CC1 disappear at the rather low field of $\sim$2 T.

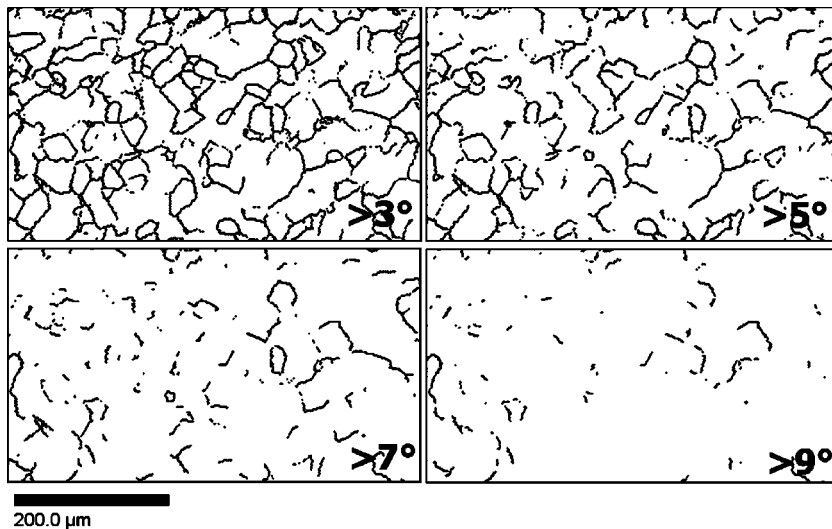Figure 2 presents the electric field–current density (*E-J*)



FIG. 3. Orientation mapping by EBSD on the Ni-W substrate of the bridge region of CC2. The indicated angles are the combined one-angle-common-axis misorientation.

characteristics of SC, CC1, and CC2 at 77 and 65 K. SC exhibits typical intragrain $E$-$J$ characteristics. CC1 shows rather single-crystal-like $E$-$J$ characteristics, as also, perhaps more surprisingly, does CC2. In fact there was no evidence of significant GB dissipation in the $E$-$J$ curves of CC2, in spite of its strongly reduced $J_c$ values.

Figure 3 shows the results of grain orientation mapping on the Ni-W substrate in the bridge region of CC2. The indicated angles ($\theta$) are the combined one-angle-common-axis misorientation. The grain boundary network is almost completely developed for $\theta$ values of 3°, while at 7° most apparent grain boundaries are disconnected segments. Quite a few $\theta$ values exceed 9°, but these GB segments are even more isolated. Note that these misorientation angles are between grains on the Ni-W substrate, not on the YBCO. From x-ray measurements on this sample, we observed that the in-plane texture worsened slightly from 5.9° on the Ni-W to 6.1° on YBCO, while the out-of-plane texture improved from 7.2° from 6.6°.

## IV. INFLUENCE OF THE NUMBER OF GRAINS WITHIN THE BRIDGE WIDTH

The influence of the number of grains within the bridge width was investigated with a second sample of the better-textured CC1. The $\Delta\phi$ and $\Delta\omega$ of the YBCO layer on this sample were 5.9° and 3.8°, respectively. $T_c$ was 91 K, and $J_c$ was 2.6 MA/cm$^2$ at 77 K and self-field.

The $J_c(H)$ characteristics for four different track widths varying from 380 to 48 μm at 50, 65, 77, and 85 K are shown in Fig. 4(a). There is a noticeable reduction in $J_c$ at low magnetic fields as the track width is reduced, while all tracks behave identically beyond a crossover field ($H^{cr}$) shown by the dashed line. This crossover field is surprisingly low, only 2 T at 77 K, rising to about 4 T at 50 K. The open symbols are data for the single crystalline film. They show excellent agreement with the $J_c$ curves of CC1 beyond the crossover field. The small high-field difference at 77 and 65 K is again due to the higher $T_c$ of the single crystalline sample, an effect which becomes less pronounced as temperature decreases. Figure 4(b) expands the scale at low fields to emphasize the differences between the different track widths. The two wider bridges—380 μm and 190 μm width—are always identical, regardless of field and temperature and have only a slightly reduced $J_c$ for $H < H^{cr}$ with respect to the single crystalline film. However, the 85-μm wide bridge does show a reduced $J_c$, while the 48-μm wide bridge exhibited even more reduced $J_c$ below the crossover field. For example, the 85 μm wide bridge shows about 35% reduced $J_c$ (self-field) compared to the wide bridges and the 48 μm wide bridge about 50% reduced $J_c$ (self-field).

The $E$-$J$ characteristics were extensively measured as shown in Fig. 5. The $E$-$J$ characteristics of the two wide bridges are identical regardless of temperature and magnetic fields as already implied by their identical $J_c(H)$ behavior in Fig. 4. (Note that some of the self-field data for the widest bridge do not exist, because of the 10 A current limit of the experiment.) The $E$-$J$ characteristics of the two wide bridges are also similar to those of the single-crystalline sample; nei-
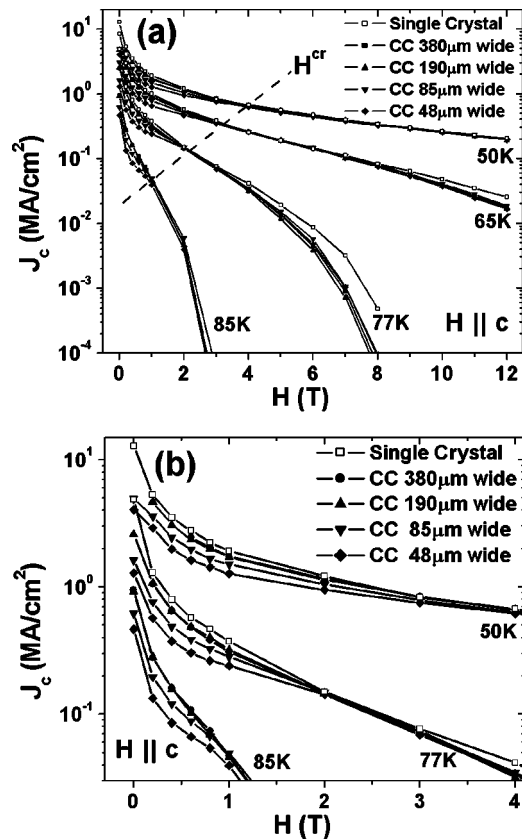


FIG. 4. (a) $J_c(H)$ for four different widths at 50, 65, 77, and 85 K up to 12 T. There is a noticeable reduction in $J_c$ at low magnetic fields as the track width is reduced, while all tracks behave identically beyond a crossover field indicated with a dashed line. This crossover field is surprisingly low, only 2 T at 77 K, rising to about 4 T at 50 K. (b) This expands the scale at low fields to emphasize the differences between the different track widths. The 65 K data are omitted to avoid overlapping. The two wider bridges—380 and 190 μm widths—are identical, while the narrower bridges exhibit reduced $J_c$.

ther set exhibits any significant GB dissipation signature. However, the two narrow bridges show a distinct broadening of the $E$-$J$ characteristics at low voltage, typical of additional GB dissipation occurring in the narrower links. The 48-μm wide bridge shows this GB dissipation more extensively than the 85-μm wide bridge. However, the GB dissipation signature progressively weakens as the applied magnetic field increases, and disappears beyond the crossover field, $H^{cr}$.

Figure 6(a) shows the results of grain orientation mapping on the Ni-W substrate in the bridge regions. Some $\theta$ values exceed 9°: however, such GB segments are always isolated ones. If the misorientation criterion is reduced to 3°, virtually all GB segments are linked, while at 5° many terminating GB segments appear. Note that these misorientation angles are between grains on the Ni-W substrate, not on YBCO. From x-ray measurements on this sample, we observed that the in-plane texture worsened slightly from 5.2° on the Ni-W to 5.9° on the YBCO, while the out-of-plane texture improved significantly from 6.0° to 3.8°.

To understand better the source of the dissipation in the narrower tracks we performed magneto-optic (MO) imaging.
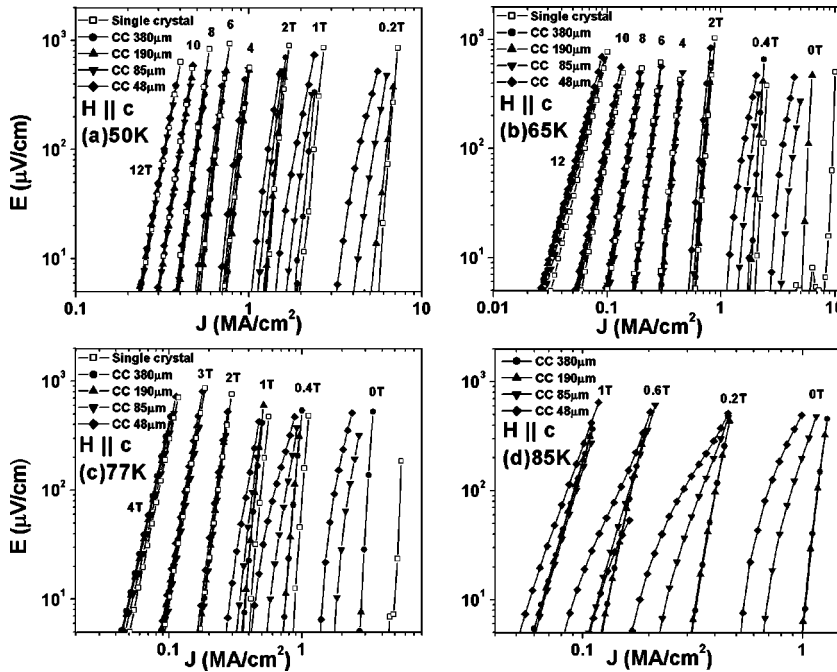
FIG. 5. *E-J* characteristics at (a) 50, (b) 65, (c) 77, and (d) 85 K. Open symbols are normalized data of the single crystalline film. Little GB dissipation signature is seen for the wider bridges, while GB dissipation signature is seen for the narrower bridges at low fields. The GB dissipation signature progressively weakens as field increases.

The MO images were taken in the field-cooled condition in 60 mT at 10 K so as to emphasize any GB-current-limiting effects. The image shown in the middle of Fig. 6 shows that only a few GBs with lower $J_c$ than the grains appear in the 48-μm wide track and only one completely crosses the track. As noted later, the misorientation of this single GB is rather high.

We also observed a second bridge set cut on other regions of the same sample, whose width was successively narrowed from 450 to 55 μm. In this case, no width dependence at all of either $J_c(H)$ or the *E-J* curves was seen, even down to the 55-μm wide bridge, as is shown in Fig. 7. The EBSD maps on the Ni-W substrate (Fig. 8) show several GBs with $\theta > 7°$ in the narrowest bridge, making it especially interesting that the *E-J* characteristics lack the grain boundary dissipation signature [Fig. 7(b)].

## V. DISCUSSION

A key issue for understanding the attainable critical current density of coated conductors is first to understand the range of fields and temperatures over which $J_c$ is reduced by the grain boundary network. The present work suggests several ways in which the GB network and its misorientation distribution can control $J_c$ given that a CC is generally many grains wide and presents a complex set of series-parallel current paths defined by obstacles around which current flows percolatively. The recent study of a RABiTS conductor by Fernandez *et al.*[19] was clearly able to distinguish the domain in which the GBs controlled $J_c(H,T)$ in their conductor. They found a non-Ohmic linear differential (NOLD)-like signature in the *E-J* curves of their 6–7 grain wide conductor and a power-law dependence of $J_c(H,T)$ when GBs controlled $J_c$ and an exponential dependence without any NOLD-like signature when flux pinning within the grains controlled $J_c$. At 77 K this crossover occurred at about 4 T

and a current density of 0.01 MA/cm$^2$. Our study nicely complements theirs because the FWHM of the YBCO of their conductor was ~8°, rather larger than our three samples.

It is clear from comparing the $J_c$ and FWHM data in Table I that the FWHM exercises a powerful effect on $J_c$. $J_c$ (77 K, 0 T) rises from 0.3 MA/cm$^2$ ($\Delta\phi$ FWHM 8°) through 0.9 MA/cm$^2$ (6.6°) through 2.4 MA/cm$^2$ (5.5°) to 5.3 MA/cm$^2$ for the single crystal. At 1 T where the GB network influence is somewhat reduced for all three CC, the respective $J_c$ values are 0.04, 0.11, 0.36, and 0.41 MA/cm$^2$. At 77 K the crossover field $H^{cr}$ at which the GB and intragrain $J_c$ become identical was 4 T for Fernandez *et al.* ($\Delta\phi_{YBCO} \sim 8°$), while curiously no crossover was seen for our CC2 ($\Delta\phi_{YBCO} \sim 6.6°$). For the better-textured CC1 ($\Delta\phi_{YBCO} \sim 5.5°$), a crossover from GB to grain control was observed at ~2 T at 77 K. As FWHM values of YBCO layers have come down in recent years, e.g., 4.5° on RABiTS[21] and 2.5° on IBAD-MgO,[21] the possibility of real single-crystal-like behavior on CC indeed increases.

A second significant difference between the conductor of Fernandez *et al.*[19] and ours was that they saw the NOLD-like signature of GB dissipation very widely, while we saw this signature only when we narrowed the bridge to 1–2 grains wide, as shown in Fig. 5. In our ~7 grain wide bridges, no NOLD-like signature was visible in either CC1 or CC2 at any field or temperature. More explicitly, we did not observe any NOLD-like signature even for the narrowest track of the second bridge set, which contains several GBs with $\theta$ higher than 7° (Fig. 8).

The collective behavior observed in our two studies can be summarized briefly as follows. (1) The highest $J_c$ values were seen in the single crystals where no grain boundaries are present. In spite of much data that show significant degradation of $J_c$ with increasing thickness,[22–27] $J_c$ (77 K, 0 T) was much higher for the 1-μm-thick MOD film than for the
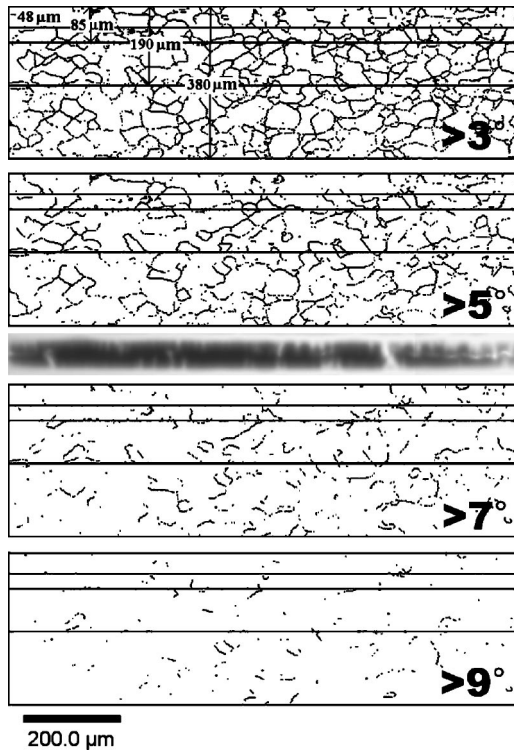
FIG. 6. Orientation mapping by EBSD on the Ni-W substrate of the bridge region. The indicated angles are the combined one-angle-common-axis misorientation. Field-cooled magneto-optic image on the narrowest bridge region is shown in the middle. Only a few GBs width lower $J_c$ than the grains appears in the narrowest bridge and only one completely crosses the track.

0.2-μm-thick pulsed laser deposition (PLD) film of Fernandez *et al.*, 5.3 vs 2 MA/cm$^2$. The lower $J_c(H,T)$ properties of the PLD CC were seen at all fields—for example at 4 T and 77 K ($H^{cr}$ for the PLD CC), $J_c$ was ~0.01 MA/cm$^2$ compared to 0.05 MA/cm$^2$ for the MOD single crystal film. (2) Although the crossover from GB to grain control of $J_c$ is clearly seen in the *E-J* curves for the wide-bridge PLD CC,[19] no crossover in the *E-J* curves is seen for the higher $J_c$ MOD coated conductors. We did see a distinctive GB signature when we narrowed the track to one or two grains but the influence on the MOD-CC *E-J* curves was much less strong than in the PLD-CC, as can be seen by comparing our Fig. 5 to Fig. 4 of Ref. 19. However, we were able to see the crossover from GB to grain control by comparison of the $J_c(H,T)$ of the single crystal to CC1 and especially in the narrow track $J_c(H,T)$ data taken on CC1.

An overview of the GB misorientation distributions in the Ni-W templates of CC1 and CC2 is given in Fig. 3 (CC2) and Figs. 6 and 8 (CC1). It is clear for both CC1 and CC2 that a major change in connectivity occurs at misorientations between 5° and 7°. At 5° or less the GB network is essentially complete so that long-range current flow must cross this whole grain boundary network. However, if only grain boundaries with $\theta > 7°$ are considered, then continuous current paths exists which do not cross the GB network, although current would still be obstructed by the set of predominantly disconnected GB segments appear that would be
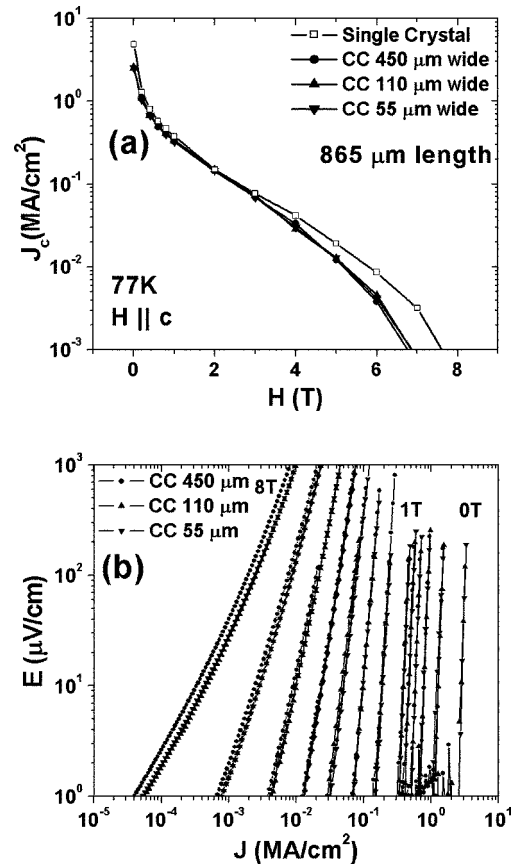


FIG. 7. (a) $J_c(H)$ and (b) *E-J* characteristics at 77 K of a second bridge set cut on other regions of the same sample. No width dependence at all of either $J_c(H)$ or the *E-J* curves was seen. The *E-J* characteristics lack the grain boundary dissipation signature.

expected to act as partial obstacles with strong dissipation at their ends.[28,29] If we reduce these $\theta$ values by 1°–2° to account for the usual orientation improvement on YBCO growth, the critical change appears to occur at about 5°–6° of YBCO misorientation for both conductors, although it does appear that the obstacle density at this $\theta$ is visibly greater in CC2 than in CC1. This conclusion is made even more explicit by the magneto-optical image in Fig. 6. In this case, only one grain boundary shows up as having a lower $J_c$ than the rest of the track. The majority of this visible GB has $\theta_{\text{Ni-W}} > 7°$ and a small portion greater than 9°. Many small segments with the same misorientations exist in the track but do not show up at all or just as partial penetrations.

The result of many bicrystal studies of YBCO grown by PLD on SrTiO$_3$ or YSZ bicrystals is that the critical angle is 3°–4°.[7,8,10] Thus a substantial GB signature and reduced $J_c$ would be expected from all three coated conductors. But, only the PLD-RABiTS conductor shows NOLD-like signature, although all three do show a $J_c$ reduction at zero field and 77 K.

In considering the role of grain boundaries in controlling $J_c(H,T)$ of coated conductors it has generally been assumed that data taken on 200–400-nm-thick films grown generally by PLD on SrTiO$_3$ or YSZ bicrystal substrates are equally valid for 1–2-μm-thick coated conductors. Indeed a number of modeling studies take this input and use it to compute the
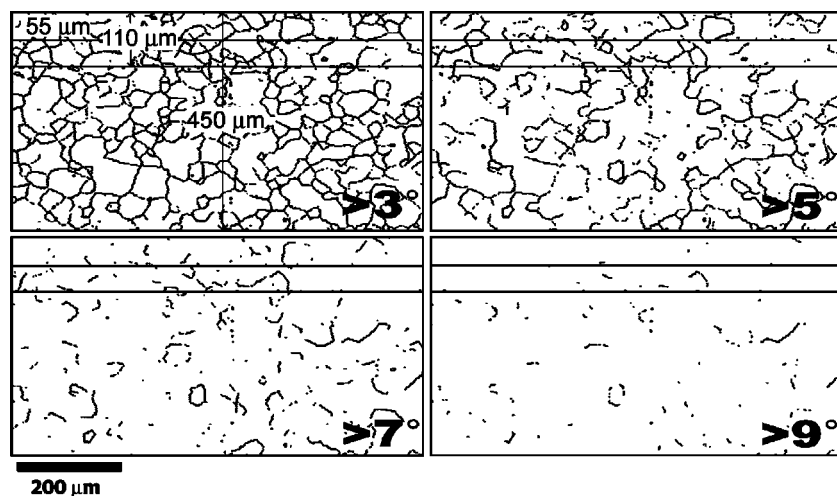
FIG. 8. Orientation mapping by EBSD on the Ni-W substrate of the second bridge region. Several GB angles are higher than 7° in the narrowest track.

critical current of long conductors as a function of their FWHM distributions.[16–18] But several prior experiments have shown that the influence of grain boundaries is complex. The fact that the ratio of $J_{gb}/J_g$ depends on field is attested by multiple studies.[7,10,13] More recently Durrell *et al.*[30] have shown that the angle made by the magnetic field to the grain boundary plane affects both the magnitude of $J_{gb}$ and the appearance of the distinctive NOLD GB signature. When the field lay within the GB plane of their 4.9° [001] tilt bicrystal, a distinctive NOLD signature and reduction of $J_{gb}$ was found. However, when they placed the magnetic field within the *ab* plane and rotated *H* with respect to the grain boundary plane which lay parallel to the *c* axis, they found that $J_{gb}$ was neither reduced nor was there any NOLD signature when the field deviated by more than ~30° from the GB plane. The NOLD signature is developed both by the distortion of vortex core structure produced by depressed superconductivity at the GB[11] and by alignment of the vortices in the GB so that a channel of weakly pinned hybrid Abrikosov-Josephson vortices is depinned at a rather sharp value of Lorentz force. Durrell's observation develops this model for the case where the field makes an angle to the GB so that only a small segment of any one vortex possesses a weakly pinned GB segment. Evidently the intragrain components of such vortices are sufficient to pin the GB segments, removing the NOLD signature in the *E-J* curve and enhancing $J_{gb}$.

The geometry of the present case is different from that of Durrell *et al.*[30] In our case all testing was done in the usual way with field parallel to the *c* axis. But recent observations by Feldmann *et al.*[31] and Holesinger *et al.*[32] show that thick MOD films have grain boundaries which do not grow vertically, but at oblique angles that are often as small as 10°–15° to the substrate. Thus the conditions of the Durrell experi-

ment can be frequently fulfilled in these MOD conductors too. Experiments to test this hypothesis explicitly are currently in progress.

In summary we have made extensive measurements of the *E-J* characteristics of recent 1-μm-thick MOD conductors and compared them to the earlier study of an 0.2-μm-thick PLD conductor.[19] We find that the influence of $\Delta\phi$ on $J_c$ is highly nonlinear, $J_c$ *(77* K, *0* T*)* rising by more than eight times as the FWHM of $\Delta\phi_{YBCO}$ decreases only from 8° to 5.5°. This is very good news for the technology of coated conductors because it makes it clear that the critical angle is significantly greater than found in previous, significantly thinner scientific bicrystal studies.[5–11] The second striking result is that the MOD coated conductors do not possess the strongly dissipative NOLD signature familiar from thin PLD films[7,9,10,19,30] and that, even when we were able to conclusively identify a dissipative GB, its misorientation was much larger than expected (~6°) and the NOLD signature was very attenuated. Thus although the low field performance of these high-$J_c$ coated conductors is still limited by grain boundaries, the effects appear to be much less than should be expected from the FWHM distributions. The dream of processes that could make single crystal properties at essentially infinite length is indeed close.

[1] M. F. Chisholm and S. J. Pennycook, Nature (London) **351**, 47 (1991).

[2] N. D. Browning, J. P. Buban, P. D. Nellist, D. P. Norton, M. F. Chisholm, and S. J. Pennycook, Physica C **294**, 183 (1998).

[3] Y. M. Zhu, J. M. Zuo, A. R. Moodenbaugh, and M. Suenaga, Philos. Mag. A **70**, 969 (1994).

[4] S. E. Babcock, X. Y. Cai, D. C. Larbalestier, D. H. Shin, N. Zhang, H. Zhang, D. L. Kaiser, and Y. F. Gao, Physica C **227**, 183 (1994).

[5] D. Dimos, P. Chaudhari, J. Mannhart, and F. K. Leoues, Phys. Rev. Lett. **61**, 219 (1988).

[6] D. Dimos, P. Chaudhari, and J. Mannhart, Phys. Rev. B **41**, 4038 (1990).

[7] D. T. Verebelyi, D. K. Christen, R. Feenstra, C. Cantoni, A. Goyal, D. F. Lee, M. Paranthaman, P. N. Arendt, R. F. DePaula, J. R. Groves, and C. Prouteau, Appl. Phys. Lett. **76**, 1755 (2000).

[8] D. M. Feldmann, D. C. Larbalestier, D. T. Verebelyi, W. Zhang, Q. Li, G. N. Riley, R. Feenstra, A. Goyal, D. F. Lee, M Paranthaman, D. M. Kroeger, and D. K. Christen, Appl. Phys. Lett. **79**, 3998 (2001).

[9] N. F. Heinig, R. D. Redwing, J. E. Nordman, and D. C. Larbalestier, Phys. Rev. B **60**, 1409 (1999).

[10] A. Diaz, L. Mechin, P. Berghuis, and J. E. Evetts, Phys. Rev. B **58**, R2960 (1998).

[11] A. Gurevich, M. S. Rzchowski, G. Daniels, S. Patnaik, B. M. Hinaus, F. Carillo, F. Tafuri, and D. C. Larbalestier, Phys. Rev. Lett. **88**, 097001 (2002).

[12] B. Holzapfel, D. Verebelyi, C. Cantoni, M. Paranthaman, B. Sales, R. Feenstra, D Christen, and D. P. Norton, Physica C **341**, 1431 (2000).

[13] A. A. Polyanskii, A. Gurevich, A. E. Pashitski, N. F. Heinig, R. D. Redwing, J. E. Nordman, and D. C. Larbalestier, Phys. Rev. B **53**, 8687 (1996).

[14] J. E. Evetts, M. J. Hogg, B. A. Glowacki, N. A. Rutter, and V. N. Tsaneva, Supercond. Sci. Technol. **12**, 1050 (1999).

[15] B. Holzapfel, L. Fernandez, F. Schindler, B. de Boer, N. Reger, J. Eickemeyer, P. Berberich, and W. Prusseit, IEEE Trans. Appl. Supercond. **11**, 3872 (2001).

[16] N. A. Rutter, B. A. Glowacki, and J. E. Evetts, Supercond. Sci. Technol. **13**, L25 (2000).

[17] E. D. Specht, A. Goyal, and D. M. Kroeger, Supercond. Sci. Technol. **13**, 592 (2000).

[18] Y. Nakamura, T. Izumi, and Y. Shiohara, Physica C **371**, 275 (2002).

[19] L. Fernandez, B. Holzapfel, F. Schindler, B. de Boer, A. Attenberger, J. Hanisch, and L. Schultz, Phys. Rev. B **67**, 052503 (2003).

[20] M. W. Rupich, U. Schoop, D. T. Verebelyi, C. Thieme, W. Zhang, X. Li, T. Kodenkandath, N. Nguyen, E. Siegal, D. Buczek, J. Lynch, M. Jowett, E. Thompson, J. S. Wang, J. Scudiere, A. P. Malozemoff, Q. Li, S. Annavarupu, S. Cui, L. Frizemeier, B. Aldrich, C. Craven, F. Niu, R. Schwall, A. Goyal, and M. Paranthaman, IEEE Trans. Appl. Supercond. **13**, 2458 (2003).

[21] X. Li, M. W. Rupich, W. Zhang, N. Nguyen, T. Kodenkandath, U. Schoop, D. T. Verebelyi, C. Thieme, M. Jowett, P. N. Arendt, S. R. Foltyn, T. G. Holesinger, T. Aytug, D. K. Christen, and M. P. Paranthaman, Physica C **390**, 249 (2003).

[22] S. R. Foltyn, P. Tiwari, R. C. Dye, Q. Le, and X. D. Wu, Appl. Phys. Lett. **63**, 1848 (1993).

[23] X. D. Wu, S. R. Foltyn, P. Arendt, J. Townsend, I. H. Campbell, P. Tiwari, Q. X. Jia, J. O. Willis, M. P. Maley, J. Y. Coulter, and D. E. Peterson, IEEE Trans. Appl. Supercond. **5**, 2001 (1995).

[24] S. R. Foltyn, Q. X. Jia, P. N. Arendt, L. Kinder, Y. Fan, and J. F. Smith, Appl. Phys. Lett. **75**, 3692 (1999).

[25] B. W. Kang, A. Goyal, D. R. Lee, J. E. Mathis, E. D. Specht, P. M. Martin, D. M. Kroeger, M. Paranthaman, and S. Sathyamurthy, J. Mater. Res. **17**, 1750 (2002).

[26] K. J. Leonard, A. Goyal, D. M. Kroeger, J. W. Jones, S. Kang, N. Rutter, M. Paranthaman, D. F. Lee, and B. W. Kang, J. Mater. Res. **18**, 1733 (2003).

[27] D. M. Feldmann, D. C. Larbalestier, R. Feenstra, A. A. Gapud, J. D. Budai, T. G. Holesinger, and P. N. Arendt, Appl. Phys. Lett. **83**, 3951 (2003).

[28] A. Gurevich and M. Friesen, Phys. Rev. B **62**, 4004 (2000).

[29] D. Abraimov, D. M. Feldmann, A. A. Polyanskii, A. Gurevich, G. Daniels, D. C. Larbalestier, A. P. Zhuravel, and A. V. Ustinov, Appl. Phys. Lett. **85**, 2568 (2004).

[30] J. H. Durrell, M. J. Hogg, F. Kahlmann, Z. H. Barber, M. G. Blamire, and J. E. Evetts, Phys. Rev. Lett. **90**, 247006 (2003).

[31] D. M. Feldmann (private communication).

[32] T. G. Holesinger (private communication).